DESIGN AND PARAMETER OPTIMIZATION OF A PNEUMATIC AIR-JET PRE-SEPARATION MECHANISM FOR TRANSPLANTING
/
用于移栽的气流冲击式钵苗预分离装置的设计与参数优化

Mengqi ZHANG [1),2)], Bolong WANG [1),2),*], Fangyuan LU [1),2),*], Guohai ZHANG [1),2)], Xiangyu WU [1),2)], Xiang REN [1),2)], Yaxin SONG [1),2)]

[1)] School of Agricultural Engineering and Food Science, Shandong University of Technology, Zibo / China;
[2)] Institute of Modern Agricultural Equipment, Shandong University of Technology, Zibo / China;
Tel: +8615288942032; +8613581044910; E-mail: lufangyuan11@163.com; wang1988-1226@163.com
First corresponding author: Fangyuan LU; Second corresponding author: Bolong WANG
DOI: https://doi.org/10.35633/inmateh-78-103

Keywords: *Precision agriculture, Transplanter automation, Air-jet seedling ejection, Seedling pre-separation, Substrate adhesion force, Jet impact force*

ABSTRACT
To address the issues of high damage rates and low success rates in seedling picking due to adhesion between seedlings and pots in the picking mechanism of an automatic transplanter, this study proposes a pre-separation method for pot seedlings based on airflow impact. Unlike the traditional jacking or vibrating-assisted separation method, this method achieves pre-separation through non-contact airflow impact and minimizes mechanical damage to the root-soil composite. Based on this method, a seedling pre-separation mechanism was designed and integrated into the seedling picking mechanism. By establishing a mechanical model of the airflow impact force, the influence of the nozzle aperture and air pressure on the separation effect was revealed. Parameter optimization and functional verification were completed using 50-day-old tomato seedlings. Experimental results showed that the pre-separation success rate of pot seedlings was 93.3% under the optimal combination of a 5 mm nozzle aperture and 125 kPa air pressure. After integration into the seedling pick-up mechanism, the pick-up success rate was 94.4%, with a damage rate of only 1.4%. This study confirmed that air-blowing pre-separation technology can effectively eliminate adhesion between pot seedlings and their pots, significantly reducing damage to seedlings and providing a feasible technical solution for developing a low-damage, automatic transplanter seedling pick-up mechanism.

摘 要
为解决全自动移栽机取苗机构因钵苗-钵体间黏附力导致的高损伤率和低取苗成功率的问题，本研究提出一种基于气流冲击的钵苗预分离方法。与传统的顶杆式或振动式辅助分离方式不同，该方法通过非接触式气流冲击实现预分离，最大限度减少对根土复合体的机械损伤。据此设计了钵苗预分离机构，并将其集成应用于取苗机构中。通过建立气流冲击力的力学模型，揭示了喷嘴孔径与气压对分离效果的影响规律。以 50 天龄番茄育苗盘苗为对象，完成了参数优化与功能验证。试验结果表明，在喷嘴孔径 5 mm、气压 125 kPa 的最优组合下，该装置的钵苗预分离成功率达 93.3%；集成于取苗机构后，取苗成功率为 94.4%，损伤率仅为 1.4%。本研究证实气吹预分离技术能有效消除钵苗与钵体间的黏附力，显著降低幼苗损伤率，为开发低损伤型全自动移栽机取苗机构提供了可行的技术路径。

INTRODUCTION
Seedling transplanting is a key phase in vegetable production, helping to shorten the crop growth period while improving yield and quality (*Khadatkar et al., 2018*). Most vegetable transplanters in China are semi-automatic, requiring manual seedling selection and transfer. This is inefficient and falls short of the need for full mechanization. Therefore, there is an urgent demand for fully automatic vegetable transplanters capable of automated seedling picking and dropping. The core challenge lies in the design and optimization of the seedling picking mechanism (*Cheng et al., 2024, Xu et al., 2025*). Extensive research on this mechanism has been conducted by scholars both domestically and internationally. Current studies primarily focus on two types: stem clamping and plug clamping. Despite significant progress, the damage rate for plug seedlings remains considerably higher compared to manual operation (*Choi et al., 2024, Ye et al., 2020, Yue et al., 2022, Islam et al., 2020, Ali et al., 2025)*. Damage mainly occurs during the separation of the seedling from the plug.

To overcome the adhesion between them and ensure smooth removal, the picking mechanism must apply a substantial clamping force. However, this can damage the seedling stem and substrate, adversely affecting the mechanism's performance (*Zhou et al., 2024, Li et al., 2015, Wang et al., 2015*).

The core issue of reducing seedling damage has been the focus of extensive research by scholars both domestically and internationally, with studies undertaken from a variety of technical perspectives (*Hu et al., 2022, Han et al., 2025, Wang et al., 2021, Khadatkar Abhijit et al., 2023, Paudel et al., 2024*). The mainstream solutions fall into two categories. Firstly, the push rod-assisted separation type. In this method, prior to the clamping of the seedling claw, the seedling is pre-ejected from the cell by the push rod. This process serves to eliminate the adhesion between the plug seedling and the cell (*Zhang et al., 2024, Ren et al., 2022*). For instance, the FUTURA (Maranello, Italy) transplanting machine developed by the Italian company FERRARI utilizes a top clamping combination method. This method involves the pneumatic push rod lifting the plug seedling in advance, and the clamping mechanism then completes the seedling pick-and-drop operation. *Peng et al.,* (*2025*) also designed a push rod combined with a seedling picking device. Following experimental verification, the damage rate of plug seedlings was found to be 4.17%, and the substrate loss rate was 6.07%. A second method is the vibration-assisted stripping type, in which the adhesion force between the plug seedling and the cell is pre-eliminated by means of vibration. For instance, *Yao et al.,* (*2022*) conceived a clamping vibration composite seedling pick-up mechanism. In the operation, the plug seedlings were initially loosened by the vibration device and subsequently clamped.

Although push-rod-assisted separation can reduce damage to some extent, the hard contact between the push rod and the substrate can cause a substrate loss rate. Vibration-assisted methods, while effective in reducing adhesion, often involve complex control strategies and may affect root system stability. These limitations highlight the need for a non-contact, controllable, and low-damage pre-separation solution. To address these limitations, this study proposes a novel air-jet pre-separation method. In this method, the instantaneous impact force is generated by the airflow acting on the base of the seedling, enabling it to be separated smoothly without mechanical contact. Compared with the 'push rod-assisted separation type' and the 'vibration-assisted stripping type', the airflow pre-separation scheme responds quickly, is gentle, and can be controlled, greatly reducing damage to the root-soil composite during the separation process. This paper presents a pre-separation mechanism for pot seedlings based on airflow impact, with the operating parameters of the mechanism optimized through a combination of theory and experimentation. This study offers a novel solution and technical reference for a low-damage clamping device for pot seedlings in an automatic vegetable transplanter.

MATERIALS AND METHODS

Design and Optimization Logic of Plug Seedling Pre-Separation Mechanism

This study aims to design and implement a plug seedling pre-separation mechanism that can generate a controllable airflow impact force, based on the airflow impact pre-separation method. To achieve this, the research follows a systematic methodology involving the design of the mechanism scheme and parameter optimization.

The design of the mechanism includes the design of the hardware and software. The hardware design primarily involves the structural design and layout of each component of the pot seedling pre-separation mechanism. The software design covers the control of each component's actions and the timing of their interactions during operation. Together, they ensure the normal operation of the seedling pre-separation mechanism.

After completing the structural design of the plug seedling pre-separation mechanism, its parameters should be optimized to ensure effective operation. Mechanical analysis of the mechanism in operation reveals the key force that determines the separation effect, providing insight into the parameter optimization factors and their influence on the separation effect. Finally, by combining theoretical analysis with experimentation, the optimal combination of parameters for the seedling pre-separation mechanism can be obtained and its operational effectiveness verified.

Design and Working Principle of Plug Seedling Pre-Separation Mechanism

Overall Design of the Mechanism

The overall structure of the plug seedling pre-separation mechanism is illustrated in Figure 1. It consists of the following components: an air blowing device, a plug tray conveying device, a tray clamping device, a photoelectric sensor, an electric control box, and others.

The mechanism incorporates both motor and pneumatic actuators and employs a modular mechatronics design. The system is controlled by a programmable logic controller (PLC), which enables the automatic operation of plug feeding, plug fixing, plug seedling pre-separation, and other processes.

The tray fixing device and the air blowing device in the seedling pre-separation mechanism are controlled by pneumatic mode, and the overall gas path design is shown in Figure 2. The fixing device utilizes a single-acting cylinder as the driving element, and controls the on-off of the gas path through two three-way solenoid valves. The air-blowing device regulates the on-off of the gas path and the pressure of the jet airflow through the solenoid valve and the pressure-regulating valve. The gas path is connected by a polyurethane gas pipe with an inner diameter of 6 mm, and the air compressor is used as the gas source to ensure a stable supply of gas in the gas path.

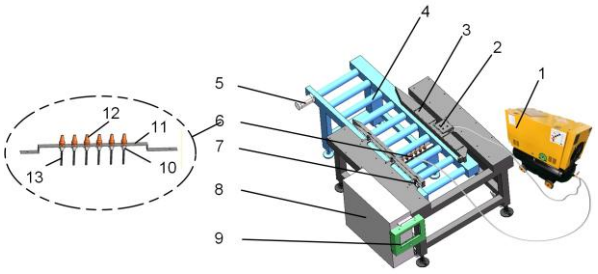

Fig. 1 - Schematic Diagram of Seedling Pre-Separation Mechanism

1. Compressor; 2. Cylinder; 3. Tray fixing device; 4. Tray conveying device; 5. Stepper motor; 6. Air-blowing device; 7. Photoelectric switch; 8. Electrical control box; 9. Touchscreen; 10. Pneumatic connector; 11. Air-blowing device mounting bracket; 12. Air nozzle; 13. Air hose.

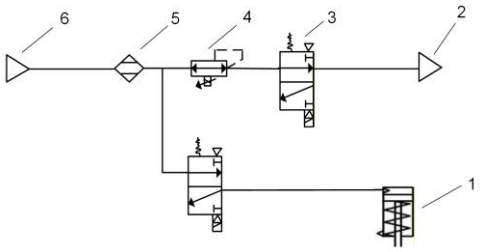

Fig. 2 - Air Circuit Diagram for Seedling Pre-Separation Mechanism

1. Single-acting cylinder; 2. Air nozzle; 3. Two-position three-way solenoid valve; 4. Pressure regulator; 5. Air dryer; 6. Air supply.

Principle of Operation

The pre-separation between the plug seedling and the cell is achieved via airflow impact. The nozzle of the air-jet device ejects a constant-pressure airflow, which strikes the bottom of the seedling through the drainage hole at the base of the plug tray. This instantaneous impact lifts the seedling. After the airflow ceases, the seedling falls back onto the cell, thereby completing the pre-separation process.

The seedling pre-separation operation involves a sequential process: tray conveying, position detection, tray clamping, and air-jet seedling ejection. During operation, a roller driven by a stepper motor conveys the tray forward until a photoelectric sensor detects that it has reached the preset working position. Once positioned, the tray clamping device is activated to secure the tray in place. Simultaneously, the air-jet device is triggered to eject a constant-pressure airflow. The plug seedlings are thus pre-separated from their cells by the impact force. The airflow lasts for 0.5 s, after which it ceases, completing a single pre-separation cycle.

Control System Design

The control system is the core component ensuring the precise operation of the seedling pre-separation mechanism, with its overall architecture shown in Figure 3. For tray position detection, a Keyence PZ-V/M series photoelectric sensor (Osaka, Japan) is employed. An SMC VQZ series high-speed solenoid valve (Tokyo, Japan) controls the pneumatic circuit for both the tray clamping device and the air-blowing device. Tray feeding is driven by a Leadshine CM series stepper motor (Shenzhen, China) paired with a DM-C series driver (Shenzhen, China). To achieve coordinated control of these actuators, a Xinjie XD3-24T4-E PLC (Jiangsu, China) is selected as the main controller. This PLC features 14 input and 10 output interfaces, with an instruction processing speed ranging from 0.02 to 0.05 μs, meeting the control accuracy and response speed requirements of the mechanism. Additionally, the system is equipped with a Xinjie touch screen (Jiangsu, China) to provide a human–machine interface (HMI), facilitating command input and fault alarm handling.

To ensure precise sequential control of the components in the seedling pre-separation mechanism, the workflow of the control system is designed as shown in Figure 4. After system startup, the Programmable Logic Controller (PLC) (Xinjie, Jiangsu, China) first performs an initialization. It then executes, according to the preset logic, a sequence of operations: tray conveying, position detection, tray clamping, and air-jet seedling ejection, thereby completing the pre-separation of a single row of plug seedlings. The system then cyclically repeats this single-row pre-separation action.

The PLC's internal counter tracks the number of rows processed, and the pre-separation for an entire tray is considered complete once the count reaches 12. After completing a full tray, the system checks whether a stop command is received. If not, it enters a standby state. Once the next tray is conveyed to the working position, the entire process repeats.

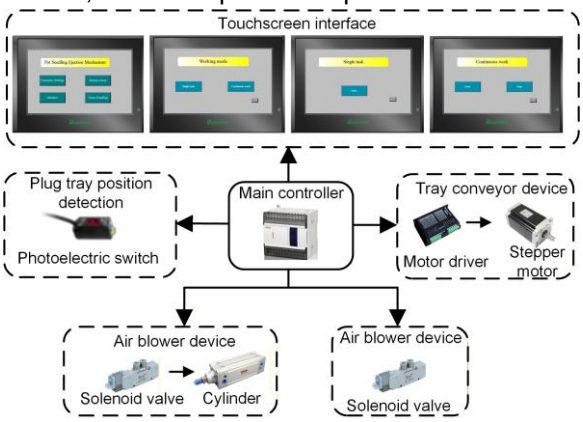

Fig. 3 - Overall Framework Diagram of the Control System

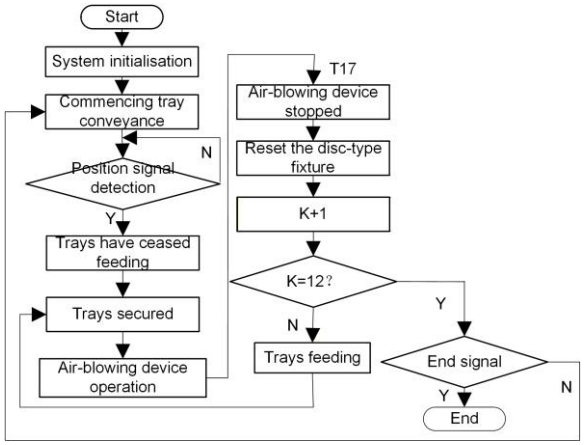

Fig. 4 - Overall Control Flowchart

Mechanical Analysis of Plug Seedling Pre-Separation Mechanism

In order to ensure the separation effect of the pre-separation mechanism of the plug seedling, the separation force of the plug seedling-cell under the airflow impact scene is explored. A substrate adhesion force is established between the plug seedling and the cell; this force is the core force that hinders the separation of the seedling from the cell. As demonstrated in Figure 5, the airflow impact force of the air-blowing device on the plug seedling must overcome the gravitational force, the adhesion force, and the friction force between the plug seedling and the cell in order to achieve the separation of the plug seedling from the cell.

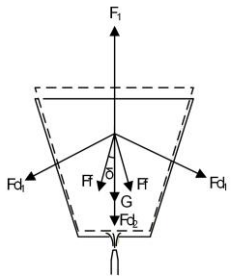

Fig. 5 - Force Analysis Diagram for Seedling-Tray Separation

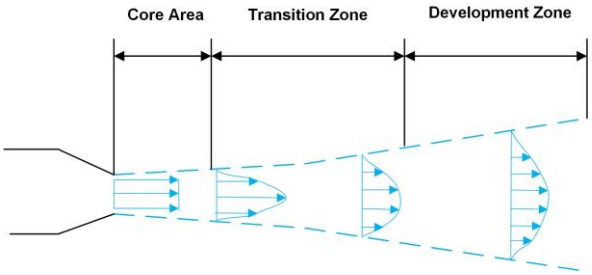

Fig. 6 - Jet Structure Diagram

As per the force analysis, the airflow impact force necessary for the plug seedling to disengage from the cell is as follows:

$$F_1 = G + 4Ff\cos\delta + 4Fd_1\sin\delta + Fd_2 \quad (1)$$

where F_1 is the airflow impact force, N; Ff is the friction force between the plug seedlings and the cell, N; G is the gravitational force exerted by the plug seedlings, N; Fd_1 is the adhesion force between the plug seedling and the cell, N; Fd_2 is the adhesion force between the plug seedling and the cell, N.

The airflow ejected from the nozzle acts on the bottom of the plug seedling through the drainage hole at the base of the cell. Given that the seedling is stationary and the ambient air is nearly still, the airflow during the pre-separation process forms a jet (*Behjat et al., 1997, Shukla et al., 2017*). A jet is a typical flow pattern in fluid mechanics, characterized by strong momentum exchange and energy dissipation between the high-speed fluid and the stationary surrounding medium. According to jet development theory, the flow field can be divided into three distinct regions: the potential core, the transition region, and the fully developed region (Figure 6). Upon exiting the nozzle, the airflow remains unaffected by the ambient air, maintaining a nearly constant velocity equal to the exit velocity. This section is known as the potential core, and its length is approximately four to five times the nozzle diameter. Beyond the potential core, the jet begins to interact intensely with the surrounding air. A large velocity gradient at the jet boundary, due to the stagnant surrounding air, entrains the ambient air into the flow. This marks the transition region, where the centerline velocity

progressively decays. Further downstream, the jet enters the fully developed region, where the flow becomes fully turbulent and exhibits chaotic, irregular motion.

As the airflow travels from the supply to the nozzle, the pressure energy is converted into kinetic energy. Assuming negligible energy loss in the circuit, the Bernoulli equation (*Cummins et al., 2017, Qin et al., 2017*) describes the energy conservation between the supply and the nozzle exit as follows:

$$\begin{cases} P_1 + \frac{\rho {v_0}^2}{2} = P_2 + \frac{\rho {v_1}^2}{2} \\ P_1 = P_0 + P_3 \\ P_2 = P_0 \\ P_3 = P_1 - P_2 \end{cases} \quad (2)$$

where P_0 is the atmospheric pressure, Pa; P_1 is the gas pressure, Pa; ρ is the airflow density (assumed to be 1.22 kg/m^3 at 25 °C standard atmospheric pressure), kg/m^3; v_0 is the air flow velocity at the air source, m/s; P_2 is the pressure at the air blowing nozzle, Pa; v_1 is the air flow velocity at the air blowing nozzle, m/s; P_3 is the number of gas path pressure, Pa.

Given that the capacity of the air supply far exceeds the nozzle flow rate, the airflow velocity at the supply can be neglected (i.e., $v_0 \approx 0$). Therefore, from Equation (5), the airflow velocity at the nozzle exit (v_1) is:

$$v_1 = \sqrt{\frac{2P_3}{\rho}} \quad (3)$$

In fluid dynamics, gas flow can be expressed in two ways: volume flow rate (Q_v), defined as the volume of gas passing through a cross-section per unit time; and mass flow rate (Q_m), defined as the corresponding mass per unit time (*Babu et al., 2021*). Due to flow resistance and turbulence, energy losses are inevitable as the air travels from the source to the nozzle, causing the actual flow rate to deviate from the theoretical value. Therefore, a correction coefficient (C_d) is introduced (*Zhu et al., 2024*). The flow rate at any given cross-section during operation is then calculated as follows:

$$\begin{cases} Q_v = A \times v \\ Q_m = C_d \times \rho \times Q_v \end{cases} \quad (4)$$

where v is the airflow velocity at the cross-section, m/s; A the cross-sectional area, m^2.

In the plug seedling pre-separation scenario, the nozzle is positioned immediately adjacent to the cell base. Consequently, when the airflow first contacts the seedling's bottom, it is still within the potential core of the jet, meaning its velocity remains equal to the exit velocity at the nozzle. When the airflow impacts the seedling's bottom axially, it transitions from axial flow to radial diffusion, causing the axial velocity to drop abruptly to zero. Therefore, the change in the axial momentum of the airflow during impact is equal to the impulse exerted on the seedling. Applying the impulse-momentum theorem, the following equation can be derived:

$$\begin{cases} I = P_{before} - P_{after} \\ I = F_1 \times \Delta t \\ P_{before} = Q_{m1} \times \Delta t \times v_2 \\ P_{after} = Q_{m2} \times \Delta t \times v_3 \\ v_2 = v_1 \\ v_3 = 0 \end{cases} \quad (5)$$

where I is impulse, N·s; P_{before} is the momentum before impact, kg·m/s; P_{after} is the momentum after impact, kg·m/s; F_1 is the impact force of airflow on the bottom of the plug seedling, N; Q_{m1} is the mass flow rate of the cross section of the airflow before the impact, kg/s; Δt is the time of action of force, s; v_2 is the axial flow velocity before the air impact on the plug seedling, m/s; Q_{m2} is the mass flow rate of the airflow after the air impact on the plug seedling, kg/s; v_3 is the axial flow velocity after the airflow impacts the plug seedling, m/s.

The substitution of the v_2 and Q_m formulas allows the formula for the impact force of the airflow on the bottom of the plug seedling to be obtained as follows:

$$F_1 = 2 \times C_d \times A_2 \times P_3 \quad (6)$$

where A_2 is defined as the range of the impact force of the airflow on the bottom of the plug seedling, m^2.

As shown in Equation (6), the airflow impact force is primarily determined by the airflow action area and the air pressure, both of which are positively correlated with the force. To ensure the smooth ejection of plug seedlings, the key parameters—namely, the nozzle aperture and the air pressure—require careful selection and optimization. The following sections detail this parameter selection process.

Air Blowing Nozzle Diameter Calculation Selection

As can be seen from the previous text, the size of the airflow impact force of the mechanism is related to the aperture of the gas nozzle and the air pressure in the gas path.

Therefore, this section begins by determining the selection range for the subsequent parameter optimization experiment through preliminary calculation of the gas nozzle aperture.

During operation, if the airflow impinges directly on the plug tray, it can cause tray displacement, edge warping, and attenuation of the impact force, all detrimental to separation. To prevent this, the nozzle diameter must be smaller than the drainage hole diameter at the cell bottom. Furthermore, upon injection, the near-stagnant air around the nozzle causes the jet to diverge due to the pressure difference, increasing its effective area beyond the nozzle aperture. Therefore, to ensure the force acts entirely on the seedling, the effective area of the diverged jet must remain smaller than the drainage hole diameter, i.e.,

$$\begin{cases} d_0 \le d_{1min} \\ d_0 = d_2 + 2l \times tan\,\alpha \end{cases} \quad (7)$$

where d_0 is the diameter of the area affected by the impact force of the airflow, mm; d_1 is the diameter of the drainage hole in the seed tray, mm; d_2 is the air nozzle diameter, mm; i is the distance between the air nozzle and the bottom of the tray, mm; α is the jet divergence angle (the fixed value is 12°25′), °.

The standard drainage hole diameter for a 72-cell tray is 7 mm. However, manufacturing tolerances introduce variation. Measurements of 20 randomly selected holes using a vernier caliper yielded a minimum diameter of 6.58 mm, a maximum of 7.46 mm, and an average of 7.02 mm. To guarantee successful ejection under all conditions, the smallest measured drainage hole diameter is used in the design calculation. This leads to the following constraint for the nozzle diameter (d_2):

$$d_2 \le 5.28 \text{ mm} \quad (8)$$

Conversely, an excessively small nozzle diameter can cause stress concentration and rupture of the seedling substrate at the impact point. Once ruptured, airflow escapes through the crack instead of providing a uniform lifting force, hindering separation. To avoid substrate damage, the effective impact area must be no less than half of the largest drainage hole diameter. This provides a lower bound:

$$d_0 \ge \frac{d_{1max}}{2} \quad (9)$$

In summary, combining these constraints gives the allowable range for the nozzle diameter as $2.41 \le d_2 \le 5.8$. Based on standard available sizes, preliminary nozzle diameters of 3, 4, and 5 mm were selected for further experimentation.

Pressure Parameter Selection Pre-Experiment

The air pressure and the air nozzle aperture affect the impact force of the airflow of the mechanism together. Based on the previously determined nozzle diameters of 3, 4, and 5 mm, preliminary experiments were conducted to identify the optimal air pressure range for each size. The test subjects were approximately 50-day-old tomato seedlings grown in 72-cell trays. The seedlings exhibited uniform growth, with no yellowing leaves and good upright posture. The moisture content of the seedling substrate was measured using a humidity monitor and found to be between 65% and 75%. As shown in Figure 7, the nozzle was positioned directly below the center of the tray's drainage hole, with a gap of approximately 3 mm from the tray bottom. During the experiment, the air pressure was gradually increased until the plug seedling successfully separated from its cell. The critical ejection pressure at that moment was recorded.

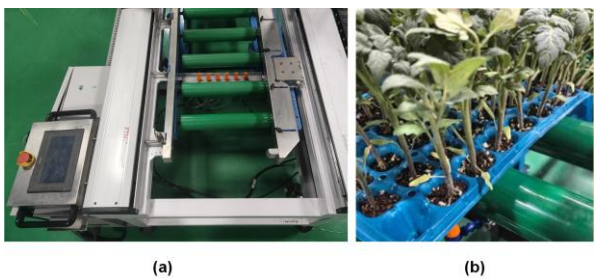

Fig. 7 - Institutions and Test Scenarios

(a) Pre-separation mechanism for seedling plugs; (b) Air nozzle layout diagram.

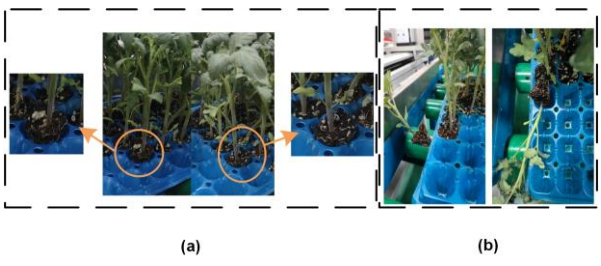

Fig. 8 - Ejection effect

(a) Successfully separated seedlings; (b) Excessive separation of seedlings.

Based on the above experimental data, a separation effect test was carried out using a 3 mm aperture air blowing nozzle under different air pressure parameters. The influence of air pressure was analyzed to determine the appropriate range of parameters for the subsequent optimal parameter combination selection test.

Optimal Parameter Combination Selection Test

In order to explore the interaction between the diameter of the air-blowing nozzle and the air pressure and select the optimal parameter combination of the seedling pre-separation mechanism, this paper conducts a full-factor experiment between the two factors of the air-blowing nozzle aperture and the air pressure. The air-blowing nozzle aperture is measured at three levels of 3, 4, and 5 mm, and the air pressure is measured at four levels of 120, 125, 130, and 135 kPa. The experiment comprises 12 parameter combinations. Each combination is replicated thrice, with the test being conducted on 30 seedlings. The test operation is analogous to the air pressure selection pre-experiment. Record the test results, and simultaneously calculate the separation success rate of seedlings Y_1, which is calculated as follows:

$$Y_1 = \frac{a}{30} \times 100\% \quad (10)$$

where a is the number of successfully separated seedlings.

After the experiment, Minitab 21 was used to analyze the variance of the test data in order to explore the impact level of various factors on the success rate of pot seedling separation. The response optimization of the test data was then carried out with the goal of achieving the maximum separation success rate in order to determine the optimal combination of parameters for the mechanism.

RESULTS

Result of Pressure Parameter Selection Pre-Experiment

The preliminary experimental findings on the pressure parameters for different apertures indicate that the critical ejection pressure of the 3 mm aperture gas nozzle is predominantly concentrated within the range of 130–135 kPa. The pressure range corresponding to the 4 mm aperture is 125–130 kPa, and the 5 mm aperture is 120–125 kPa. The experimental results are consistent with Equation 6. It can thus be concluded that, under the condition that the required airflow impact force remains constant, there is a decrease in air pressure in the gas path with an increase in gas nozzle aperture. However, this decrease is not significant. This phenomenon can be attributed to the fact that the core area of the small-aperture gas nozzle is smaller than that of the large-aperture gas nozzle. Consequently, the airflow is more likely to be disordered.

In order to explore the influence of air pressure on the separation effect of plug seedlings, an experiment was conducted. The experiment was based on a pre-experiment and used a 3 mm air-blowing nozzle. The plug seedling separation test was carried out under air pressures of 110–150 kPa. The separation effect was recorded. The test gradient was 10 kPa, and 10 plug seedlings were utilized for each air pressure. According to the final state of the seedlings after airflow, the pre-separation results can be defined as one of the following three types: ‘unseparated’, ‘successful separation’, or ‘excessive separation’, as shown in Figure 8. Unseparated plug seedlings fingers that were not lifted by the airflow or were only loosened slightly and remained in the original hole. Successful separation means that after being lifted by the airflow, the plug seedling falls back within the range of the original hole in a vertical position. Excessive separation of fingers causes the plug to be blown away from the original hole by the airflow and does not fall back into it.

The experimental results are displayed in Table 1 and Figure 9.

Table 1

Test results for 3 mm air nozzle pre-separation.

Atmospheric Pressure/kPa	Number of Unseparated Seedings	Number of Successfully Separated Seedlings	Number of Excessively Separated Seedlings
110	5	4	1
120	2	7	1
130	1	8	1
140	0	5	5
150	0	4	6

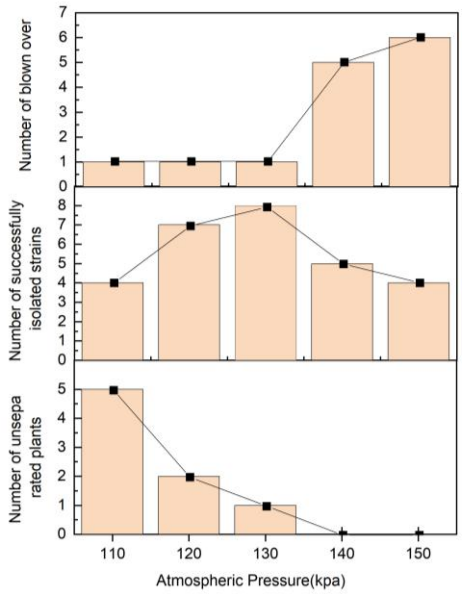

Fig. 9 - Bar Chart of Pressure-Separation Status

Table 1 presents the detailed results of the pre-separation test using a 3 mm nozzle under varying air pressures. At 110 kPa, the majority of seedlings remained unseparated, with only 3 achieving successful separation. As pressure increased to 120–130 kPa, the number of successfully separated seedlings rose to 7 and 8, respectively, while unseparated seedlings decreased to 2 and 1. This indicates that the impact force within this pressure range was sufficient to overcome adhesion without causing excessive ejection. However, at 140 kPa and above, the number of successfully separated seedlings declined sharply, while excessive separation cases increased to 5 and 6, respectively. This trend confirms the existence of a critical pressure threshold (approximately 130 kPa for the 3 mm nozzle), beyond which the impact force becomes excessive, leading to seedling over-ejection and substrate damage—consistent with the jet impact model in Eq. (6). As gas pressure increases, the impact force (F_1) rises. This increases the probability of overcoming adhesion and friction forces, increasing the initial separation success rate. However, when the threshold is exceeded, the impact force becomes too great. Excessive ejection of seedlings from the seedling block may occur, and the seedlings fail to fall back onto the seedling tray. Additionally, the high-impact force may sharply increase the shear force in the impacted area, causing rupture of the plug seedling matrix. This rupture lets airflow escape through the gap, preventing the plug seedling from producing a uniform lifting force.

The unseparated plug seedlings are vulnerable to damage during the subsequent clamping process, and the excessively separated seedlings will cause leakage. Both of these states will affect the subsequent picking and throwing of seedlings. It is evident from the experimental results that the separation effect of plug seedlings will initially improve and subsequently deteriorate with an increase in air pressure. Therefore, to ensure that the subsequent tests for optimal parameter selection encompass the critical ejection pressure values across different nozzle diameters, the pressure level range for the follow-up combinatorial tests was set at 120–135 kPa.

Result of the Optimal Parameter Combination Selection Test

The full factorial test scheme and the results of the test are displayed in Table 2.

Table 2

Full factorial trial results for the seedling pre-separation mechanism.

Serial Number	Nozzle Diameter (A)/mm	Air Pressure (B)/kPa	Number of Unseparated Seedings	Number of Successfully Separated Seedlings	Number of Excessively Separated Seedlings	Separation Success Rate
1	3	120	11	19	0	63.3%
2	3	125	9	20	1	66.7%
3	3	130	3	22	5	73.3%
4	3	135	0	20	10	66.7%
5	4	120	7	23	0	76.7%
6	4	125	5	25	0	83.3%

Serial Number	Nozzle Diameter (A)/mm	Air Pressure (B)/kPa	Number of Unseparated Seedings	Number of Successfully Separated Seedlings	Number of Excessively Separated Seedlings	Separation Success Rate
7	4	130	1	26	3	86.7%
8	4	135	0	23	7	76.7%
9	5	120	7	23	0	76.7%
10	5	125	2	28	0	93.3%
11	5	130	0	26	4	86.7%
12	5	135	0	24	6	80.0%

The experimental results were analyzed by variance analysis. The results of the analysis are presented in Table 3.

Table 3

Analysis of variance

Source	Degree of Freedom	Sum of Squares	Mean Square	F	P
Model	5	0.081	0.016	12.49	0.003**
A	2	0.060	0.030	24.13	0.001**
B	3	0.021	0.007	5.39	0.032*
Pure Error	6	0.008	0.001		
Cor Total	11	0.089			

*Note: ** indicates significant impact ($p \leq 0.05$); * indicates generally significant impact ($0.05 \leq p \leq 0.1$).*

As shown in Table 3, the significant effect of aperture A on the success rate of separation was P = 0.003, which is less than 0.05. This indicates that the effect of aperture A on the separation success rate is extremely significant. Similarly, the significance of air pressure B on the success rate of separation was P = 0.001, which is also less than 0.05 and indicates a very significant effect. These results are consistent with the previous analysis of the impact of airflow. Through regression analysis of the experimental data, the regression equation for the separation success rate was obtained.

$$Y_1 = -27.51 + 0.484A + 0.4257B - 0.0501A^2 - 0.001663B^2 \quad (11)$$

In order to select the optimal parameter combination of the plug seedling pre-separation mechanism, the response optimization was carried out with the maximum separation success rate as the target (Figure 10). The optimization results evidently show that when the aperture is set at 5 mm and the pressure is elevated to 125 KPa, the separation success rate exhibits a notable increase, reaching a maximum of 93.3%.

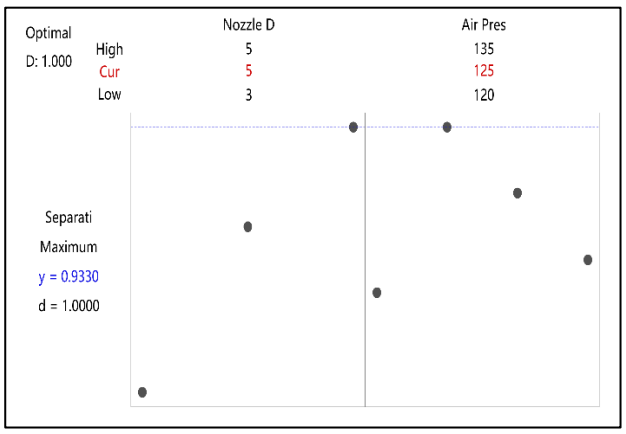

Fig. 10 - Response Optimization Chart

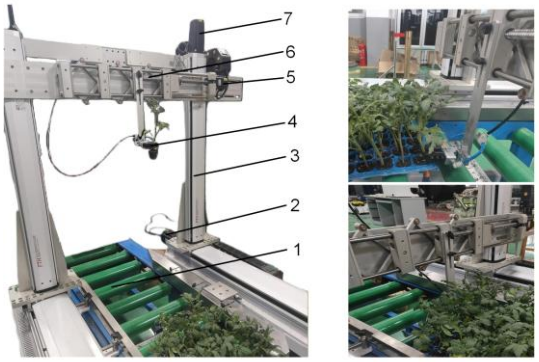

(a) (b)

Fig. 11 - Bench test

(a) Air-Blow Pre-Separation Seedling Sampling Test Bench. 1. Seedling pre-separation mechanism; 2. Stepper motor 1; 3. Linear slide module; 4. Seedling gripper; 5. Stepper motor 2; 6. Ball screw; 7. Stepper motor 3. Seedling extraction procedure.

Effect Verification Test of Plug Seedling Pre-Separation Mechanism

In order to preliminarily verify the influence of the seedling pre-separation mechanism on the operation effect of the whole seedling picking process, this paper carries out the verification test of the seedling picking effect on the air-blown pre-separation seedling picking test bench. The test bench is principally composed of the pre-separation mechanism of the plug seedling, the seedling picking claw, the sliding table module, and so forth, as illustrated in Figure 11. The test bench's operational process is outlined below. Once the plug tray has been positioned, the pre-separation mechanism of the plug seedling initiates the spraying of air, thereby facilitating the pre-separation of the plug seedling and the cell. Subsequent to the completion of the air flow injection, the seedling claw is advanced towards the seedling picking point with the objective of clamping the plug seedling. The plug seedling is then conveyed to the seedling throwing point for the purpose of seedling throwing.

The optimal parameter combination for the pre-separation mechanism of the plug seedling is determined by the following methodology. For the bench seedling test, an air blowing nozzle with a diameter of 5 mm is utilized, and the air pressure of the air path is set to 125 KPa. A tray of 72 tomato seedlings with uniform growth over 50 days was selected as the experimental subject, and all 72 seedlings in the tray were sequentially subjected to complete air-blowing pre-separation and picking operations. The test process is illustrated in Figure 11. In the experimental setup, the process of detaching plug seedlings from the cell and clamping them to the seedling point was considered a successful outcome. The seedlings exhibiting signs of damage to the plug seedling substrate or stem were designated as 'damaged seedlings'. The seedling picking success rate S_1 and the damage rate of plug seedlings S_2 were utilized as the evaluation indices of the seedling pick-up effect. The calculation formula for the evaluation indexes is as follows:

$$\begin{cases} S_1 = \frac{b}{72} \times 100\% \\ S_2 = \frac{c}{b} \times 100\% \end{cases} \quad (12)$$

where b is the number of successfully gripped seedlings; c is the number of seedlings that have been damaged in the plug;

The statistical analysis of the results of the bench test demonstrated that, under the optimal parameter combination, the separation success rate of the air-blowing pre- separation seedling test bench could reach 94.4%, and the damage rate of the plug seedling was only 1.4%.

To evaluate the performance of the air-blown pre-separation seedling picking test bench, it is compared here with the conventional seedling picking mechanism described in previous studies. Previous studies have shown that Liu et al. designed a stem-type seedling picking mechanism based on visual recognition. This mechanism achieved a seedling picking success rate of 92.9% and caused damage to 7.2% of plug seedlings (*Liu et al., 2024*). *Peng et al., (2025)* pusher-assisted seedling picking mechanism achieved a seedling picking success rate of 94.4%, with a matrix damage rate of 6.07% and a seedling damage rate of 4.17%. The seedling picking device designed by *Hu et al., (2022)* had a success rate of 94.12%, with an integrity rate of plug seedlings of 94.12%. Compared with previous studies, the mechanism proposed in this study has achieved outstanding results in significantly reducing the damage rate of plug seedlings; however, there is still room for improvement in the seedling picking success rate. Subsequent studies will optimize the operating parameters of the flexible seedling picking claws to improve the seedling picking success rate. The preliminary experiment findings demonstrate that the pre-separation process of plug seedlings can effectively address the issue of high damage rates to the seedling pick-up mechanism of the transplanter. This provides a feasible technical path and theoretical reference for the design and development of a low-damage seedling pick-up mechanism.

CONCLUSIONS

This study proposed a novel air-jet pre-separation method and designed a corresponding mechanism to address the high seedling damage caused by the adhesion between plug seedlings and their cells during automated transplanting. The main conclusions are as follows:

(1) A mechanical analysis of the pre-separation process was conducted, focusing on the airflow impact force, which determines separation success. Models for these forces were established, and their main influencing factors were investigated. The impact force is determined by the nozzle aperture and air pressure.

(2) A pre-separation mechanism was designed, and a full-factorial experiment was conducted, with nozzle aperture and air pressure as the influencing factors. Response optimization of the experimental results identified the optimal parameter combination: a 5 mm nozzle aperture and 125 kPa air pressure. Under this configuration, the separation success rate reached 93.3%.

(3) Verification tests on an air-jet pre-separation test bench showed that, under the optimal parameters, the seedling picking success rate attained 94.4% with a damage rate of only 1.4%. This demonstrates that the pre-separation mechanism can significantly reduce seedling damage during the picking operation.

The verification of operational performance for the air-blow pre-separation seedling picking test bench has so far remained at the preliminary bench test stage, and its work environment cannot fully replicate the complex conditions of field transplanting. To bridge this gap and validate the practical value of the mechanism, the core direction of subsequent research is to install a planting mechanism on the existing platform and conduct comprehensive field tests, thereby fully verifying its operational effectiveness, environmental adaptability, and sustained working reliability.

ACKNOWLEDGEMENT

This research was funded by Key Research and Development Program of Ningxia, grant number 2023BCF01052.

REFERENCES

[1] Ali, A. N., Nigus, M. G., Paramasivam, V., Petrů, J., & Čep, R. (2025). Design and Analysis of Automatic Whole Row Tomato Seedling Transplanter Technology with Integrated Controlling System. *Journal of Field Robotics*. https://doi.org/10.1002/rob.70142

[2] Babu V. (2021). Normal Shock Waves. In V. Babu (Ed.), *Fundamentals of Gas Dynamics* (pp. 25–39). Springer International Publishing. https://doi.org/10.1007/978-3-030-60819-4

[3] Behjat A., Tallents G.J., & Neely D. (1997). The characterization of a high-density gas jet. *Journal of Physics D: Applied Physics,* 30(20), 2872. https://doi.org/10.1088/0022-3727/30/20/014

[4] Cheng B., Wu H., Zhu H., Liang J., Miao Y., Cui Y., & Song W. (2024). Current status and analysis of key technologies in automatic transplanters for vegetables in China. *Agriculture*, 14(12), 2168. https://doi.org/10.3390/agriculture14122168

[5] Choi I.-J., Habineza E., Reza M.N., Park S.-H., Lee D.-H., Lee D.-H., & Chung S.-O. (2024). Theoretical kinematic analysis of a sliding-type picking mechanism for automatic pepper seedling transplanters. *Korean Journal of Agricultural Science*, 51(4), 497–511. https://doi.org/10.7744/kjoas.510408

[6] Cummins J.J., Nash C.J., Thomas S., Justice A., Mahadevan S., Adams D.E., & Barth E.J. (2017). Energy conservation in industrial pneumatics: A state model for predicting energetic savings using a novel pneumatic strain energy accumulator. *Applied Energy*, 198, 239–249. https://doi.org/10.1016/j.apenergy.2017.04.036

[7] Han L., Zhang M., Wang Y., Ma G., Yang Q., & Liu Y. (2025). Design and tests of a large-opening flexible seedling pick-up gripper with multiple grasping pins. *Agronomy*, 15(7), 1634. https://doi.org/10.3390/agronomy15071634

[8] Hu J., Liu Y., Liu W., Zhang S., Han L., & Zeng T. (2022). Experiment on combined seedling picking device with top clamping and pulling. *Transactions of the Chinese Society for Agricultural Machinery*, 53(Suppl. 1), 110–117. https://doi.org/10.6041/j.issn.1000-1298.2022.S1.012

[9] Islam M.N., Iqbal M.Z., Ali M., Chowdhury M., Kabir M.S.N., Park T., Kim Y.-J., & Chung S.-O. (2020). Kinematic analysis of a clamp-type picking device for an automatic pepper transplanter. *Agriculture*, 10(12), 627. https://doi.org/10.3390/agriculture10120627

[10] Khadatkar A., Mathur S.M., & Gaikwad B.B. (2018). Automation in transplanting: A smart way of vegetable cultivation. *Current Science*, 115(10), 1884–1892. https://doi.org/10.18520/cs/v115/i10/1884-1892

[11] Khadatkar Abhijit,Pandirwar A P & Paradkar V.(2023).Design, development and application of a compact robotic transplanter with automatic seedling picking mechanism for plug-type seedlings. *Scientific reports*,13(1),1883-1883.https://doi.org/10.1038/S41598-023-28760-4

[12] Li H., Cao W., Li S., Fu W., & Liu K. (2015). Kinematic analysis and test on automatic pick-up mechanism for chili plug seedling. *Transactions of the Chinese Society of Agricultural Engineering*, 31(23), 20–27. https://doi.org/10.11975/j.issn.1002-6819.2015.23.003

[13] Liu Z., Shi L., Liu Z., Xing J., Hu C., Wang X., & Wang L. (2024). Design and testing of a seedling pick-up device for a facility tomato automatic transplanting machine. *Sensors*, 24(20), 6700. https://doi.org/10.3390/s24206700

[14] Paudel, B., Basak, J. K., Jeon, S. W., Deb, N. C., Karki, S., & Kim, H. T. (2024). Development and field testing of biodegradable seedling plug-tray cutting mechanism for automated vegetable transplanter. *Journal of Agricultural Engineering*, 55(2).

[15] Peng Z., Yang F., Li Y., Li X., Li B., & Xu G. (2025). Design and testing of a whole-row top-loosening stem-clamping seedling extraction device for hole tray seedlings. *Agriculture*, 15(2), 165. https://doi.org/10.3390/agriculture15020165

[16] Qin R., & Duan C. (2017). The principle and applications of Bernoulli equation. *Journal of Physics: Conference Series*, 916(1), 012038. https://doi.org/10.1088/1742-6596/916/1/012038

[17] Ren L., Zhao B., Cao W., Song W., & Zhao M. (2022). Design of stretchable style pick-up device for tomato seedling transplanters. *Agriculture*, 12(5), 707. https://doi.org/10.3390/agriculture12050707

[18] Shukla A., & Dewan A. (2017). Flow and thermal characteristics of jet impingement: Comprehensive review. I*nternational Journal of Heat and Technology*, 35(1), 153–166. https://doi.org/10.18280/ijht.350121

[19] Wang C., Liu C., Li Y., Song J., Wang J., & Dong X. (2021). Design and experiment of pneumatic punching high-speed seedling picking device for vegetable transplanter. *Transactions of the Chinese Society for Agricultural Machinery*, 52(5), 35–43, 51. https://doi.org/10.6041/j.issn.1000-1298.2021.05.004

[20] Wang M., Song J., Liu C., Wang Y., & Sun Y. (2015). Design and experiment of crank rocker type clamp seedlings mechanism of vegetable transplanter. *Transactions of the Chinese Society of Agricultural Engineering*, 31(14), 49–57. https://doi.org/10.11975/j.issn.1002-6819.2015.14.007

[21] Xu T., Li X., He J., Han S., Wang G., Yin D., & Zhou M. (2025). Research progress and future prospects of key technologies for dryland transplanters. *Applied Sciences*, 15(14), 8073. https://doi.org/10.3390/app15148073

[22] Yao S., Liu J., Zeng J., Shi Q., Zhao C., & He X. (2022). Design of taking-combined-with-vibration-type seedlings unloading mechanism of vegetable transplanter. *Agricultural Equipment & Vehicle Engineering*, 60(1), 70–73. https://doi.org/10.3969/j.issn.1673-3142.2022.01.015

[23] Ye B., Zeng G., Deng B., Yang C., Liu J., & Yu G. (2020). Design and tests of a rotary plug seedling pick-up mechanism for vegetable automatic transplanter. *International Journal of Agricultural and Biological Engineering*, 13(3), 70–78. https://doi.org/10.25165/j.ijabe.20201303.5647

[24] Yue R., Hu J., Liu Y., Yao M., Zhang T., & Shi J. (2022). Design and working parameter optimization of pneumatic reciprocating seedling-picking device of automatic transplanter. *Agriculture*, 12(12), 1989. https://doi.org/10.3390/agriculture12121989

[25] Zhang N., Zhang G., Fu J., Liu W., Chen L., & Tang N. (2024). Design and experiment of the seedling pick-up device with ejecting pot-clamping stem combination. *Transactions of the Chinese Society of Agricultural Engineering*, 40(9), 50–61. https://doi.org/10.11975/j.issn.1002-6819.202309091

[26] Zhou M., Sun H., Xu X., Yang J., Wang G., Wei Z., Xu T., & Yin J. (2024). Study on the method and mechanism of seedling picking for pepper (Capsicum annuum L.) plug seedlings. *Agriculture*, 14(1), 11. https://doi.org/10.3390/agriculture14010011

[27] Zhu W., Ji X., & Wang G. (2024). Reynolds number effects in wall-bounded turbulent flows. In X. Zheng & S. Balachandar (Eds.), *Proceedings of the IUTAM Symposium on Turbulent Structure and Particles-Turbulence Interaction.* pp.196–211. Springer Nature Switzerland. https://doi.org/10.1007/978-3-031-56070-9